Environ. Sci. Technol. **1998**, *32,* 3562−3569

Transport of in Situ Mobilized Colloidal Particles in Packed Soil Columns

DANIEL GROLIMUND,[†]
MENACHEM ELIMELECH,*[,‡]
MICHAL BORKOVEC,[§]
KURT BARMETTLER,[⊥]
RUBEN KRETZSCHMAR,[⊥] AND
HANS STICHER[⊥]

Department of Geological and Environmental Sciences, Stanford University, Stanford, California 94305-2115, Department of Chemical Engineering, Environmental Engineering Program, Yale University, New Haven, Connecticut 06520-8286, Department of Chemistry, Clarkson University, Potsdam, New York 13699-5814, and Institute of Terrestrial Ecology, Swiss Federal Institute of Technology, ETH-ITO, Grabenstrasse 3, CH-8952 Schlieren, Switzerland

A systematic investigation of the transport behavior of in situ mobilized soil colloidal particles in their parent soil matrix medium is presented. Particle advection, dispersion, and deposition kinetics were studied by analysis of particle breakthrough curves as a response to short-pulse particle injections to the inlet of packed soil columns. The transport of the heterogeneous soil particles was compared to the transport of monodisperse carboxyl latex particles to further understand the various particle transport mechanisms. Results show that colloidal particles travel much faster than a conservative tracer (nitrate) due to size exclusion effects, whereby mobile colloidal particles are excluded from small pores within the soil medium. Dispersivity of the natural and latex particles was compared to that of the conservative tracer, and the results indicate that particle dispersivity is greater than the tracer dispersivity. Dispersivity of colloidal particles was shown to be essentially independent of pore water velocity, whereas tracer dispersivity increased with increasing pore water velocity due to a combination of convective and diffusive transport of tracer molecules in small pores within the soil aggregates. The effect of divalent counterions on particle deposition kinetics was also investigated by comparing the results to deposition kinetics with monovalent counterions. Particle deposition rate with Ca^{2+} was shown to be higher than with Na^{+}, and the critical deposition concentrations with Na^{+} were greater than those with Ca^{2+}. In contrast to the marked effect of ionic strength and divalent cations, changes in proton activity over more than 1 order of magnitude (from pH 4.0 to 5.5) did not have a significant effect on particle deposition kinetics. Quantitative analysis of the observed particle transport results demonstrates that the transport of the natural colloidal particles in the packed soil columns can be adequately described by the advection-dispersion equation with a first-order, irreversible deposition kinetics term.

Introduction

Colloid-facilitated transport is a potentially significant contaminant transport mechanism for strongly sorbing contaminants in soils and groundwater aquifers (*1*−*3*). Field observations suggest that concentrations of mobile colloidal particles range from less than 1 mg/L to as high as a few hundred mg/L (*3*, *4*). Laboratory experiments investigating colloid-facilitated transport have confirmed that mobile colloidal particles can enhance the transport of inorganic contaminants in natural porous media (*1*, *3*). It is very likely that colloid-facilitated transport observed in column studies with natural colloidal particles and porous media occurs in a similar fashion in the subsurface environment. In addition to facilitating the transport of contaminants, particle transport in the subsurface plays an important role in the deposition of clays in sediments (*5*) and in formation plugging due to artificial recharge or secondary oil recovery (*6*).

Predicting the susceptibility of a subsurface porous medium to colloid-facilitated transport requires the understanding of three processes, namely, the generation of mobile colloidal particles, association of contaminants with such particles, and particle transport (*2*, *3*). At the present time, only the association of contaminants with surfaces of colloidal particles can be quantitatively described with some degree of certainty. The processes of particle generation and transport in natural subsurface porous media are still poorly understood (*3*). This paper will investigate the various mechanisms governing the process of particle transport, with emphasis on the role of particle deposition.

The primary mechanisms controlling the transport of colloidal particles in subsurface porous media are particle advection, dispersion, and deposition (filtration). These are influenced by the surface chemical characteristics of the natural porous media and colloids, size and morphology of colloidal particles and granular porous media, solution chemistry, and the fluid flow field. Moreover, some of these mechanisms are closely interrelated. For instance, particle deposition is influenced by particle advection (*7*, *8*), whereas particle dispersion in porous media is directly related to fluid velocity and particle advection (*9*).

Transport of colloidal particles in porous media, in particular the mechanism of particle deposition, has been extensively studied in model systems for the past two decades. The model systems involved spherical collectors such as glass beads or well sorted sand grains as granular porous media and monodisperse suspensions of polymeric latex particles or metal oxides as model colloidal particles (*7*, *10*−*13*). These studies led to a better understanding of the role of solution chemistry, hydrodynamics, particle size, and surface chemical properties of colloidal particles and collectors in particle deposition. Such model systems were also essential to test fundamental theories of particle deposition, in particular the effect of surface interactions, on the particle deposition rate. Valuable insights were also gained from studies with model systems on the influence of other factors, such as surface charge heterogeneity and roughness on the kinetics and dynamics of particle deposition in porous media (*10*).

In contrast to the vast majority of colloidal transport investigations in model laboratory systems, particle transport

* Corresponding author phone: (203)432-2789; fax: (203)432-7232; e-mail: menachem.elimelech@yale.edu.
[†] Stanford University.
[‡] Yale University.
[§] Clarkson University.
[⊥] Swiss Federal Institute of Technology.

10.1021/es980356z CCC: $15.00
Published on Web 10/07/1998

studies with natural colloidal particles and porous media are rather scarce (*14*, *15*). Moreover, studies involving the transport of in situ mobilized colloidal particles in natural, parent subsurface porous media are virtually nonexistent. Hence, at the present time, it is not clear if findings obtained from particle transport studies in idealized model systems can be directly applied to particle transport in natural subsurface porous media. More experimental investigations with natural colloidal particles and subsurface porous media will, therefore, enhance our understanding of colloidal transport in subsurface environments.

The main goal of this paper is to conduct a systematic experimental investigation of the key mechanisms that control the transport of submicrometer-size natural colloidal particles in soils under saturated flow conditions. In situ mobilized soil colloidal particles and packed soil columns were used in this investigation. Monodisperse latex particles were also employed to explain and validate key phenomena observed from experiments with the natural colloidal particles. Based on the experimental results and quantitative analyses of particle transport in porous media, the key physical and chemical mechanisms governing the transport of natural colloidal particles in soils are delineated and discussed.

Theoretical

Transport of Colloidal Particles in Porous Media. Consider a laboratory column containing a uniform natural porous medium at saturated flow conditions and constant solution composition. Transport of colloidal particles can be described by accounting for particle advection, hydrodynamic dispersion, and deposition (filtration). The concentration of suspended colloidal particles $c(x,t)$ at a column depth x and time t follows the one-dimensional advection-dispersion equation with a sink term for particle deposition (*7*, *9*)

$$\frac{\partial c}{\partial t} = D\frac{\partial^2 c}{\partial x^2} - v\frac{\partial c}{\partial x} - kc \tag{1}$$

where v is the interstitial velocity of the colloidal particles, D is the hydrodynamic dispersion coefficient, and k is the particle deposition rate coefficient. This transport equation assumes particle deposition to follow first-order kinetics and to be irreversible. Both assumptions are justified at sufficiently low particle concentrations (i.e., no blocking or ripening) and for moderate to high ionic strengths where particle release is negligible compared to particle deposition (*7*, *10*). For a semi-infinite column initially free of colloidal particles, and a unit pulse input, eq 1 can be solved with the Laplace transform technique (*16*). The final result reads

$$c(x,t) = n_0 e^{-kt}\frac{x}{2\sqrt{\pi t^3 D}}e^{-(x-vt)^2/4Dt} \tag{2}$$

where n_0 is a normalization constant which represents the total amount of colloidal particles injected divided by the total volumetric flux. In practice, this constant can be determined by a parallel bypass experiment where the column is short-circuited.

Determination of Particle Deposition Rate Coefficient. Despite suitable approaches for model systems, none of the parameters required to describe the transport of colloidal particles in natural, heterogeneous porous media is a priori accessible by independent measurements or theoretical calculations. Therefore, the three model parameters (k, D, and v) have to be determined simultaneously from the particle breakthrough curve. Two different methods of analysis are frequently used—a direct fit of the observed particle breakthrough curve to the transport equation or the moment method.

(a) Direct Fit of the Breakthrough Curve. As a first strategy, all model parameters can be evaluated directly from the transport equation. The analytical solution of the particle transport equation, eq 2, is fitted to the observed experimental particle breakthrough curves using standard algorithms for the solution of nonlinear least-squares problems. An input to the calculation is the normalization constant n_0 determined from the bypass experiment. One can also allow for an adjustable baseline in the fitting procedure. In this work, baseline corrected experimental data were used for the fitting of the particle breakthrough curves.

(b) Moment Method. The second strategy involves analysis of the moments of the observed breakthrough curves. This procedure has already been used in the past by various authors (*7*, *10*) in the pure advection limit. The moment of order n is defined as

$$\mu_n = \int_0^\infty c(x,t)t^n \, dt \tag{3}$$

The lowest order moments can be easily determined experimentally at the column outlet ($x = L$) (*17*). Note that the determination of the moments also involves the calculation of the normalization constant n_0 from the bypass experiment. The area under the breakthrough curve is proportional to μ_0. For a conservative tracer this moment is always unity, whereas for colloidal particles this moment represents the fractional amount of colloidal particles recovered at the column outlet. The average travel time of the colloidal particles is given by the ratio μ_1/μ_0, while the width of the breakthrough curve is characterized by $\epsilon = \mu_2\mu_0/\mu_1^2 - 1$ (normalized variance, $\sqrt{\epsilon}$, corresponds to the coefficient of variation). From eq 1 these moments can be evaluated invoking Laplace transform techniques (*16*). Since we are concerned with laboratory column experiments, which are usually dominated by advection, we expand our expressions as a power series in ϵ. Applying this method, we can express the deposition rate coefficient as

$$k = -\frac{\mu_0}{\mu_1}\ln \mu_0\left(1 + \frac{\epsilon}{2}\ln \mu_0 + ...\right) \tag{4}$$

Similarly, the particle transport velocity turns out to be

$$v = \frac{L\mu_0}{\mu_1}(1 - \epsilon \ln \mu_0 + ...) \tag{5}$$

while the longitudinal dispersivity $\alpha_L = D/v$ can be written as

$$\alpha_L = \frac{L\epsilon}{2}(1 - \epsilon \ln \mu_0 + ...) \tag{6}$$

In these expressions, there is a leading term and a first-order correction term proportional to ϵ which accounts for dispersivity; all higher order contributions are neglected. The leading term in eq 4 has been commonly used to evaluate the deposition rate coefficient in similar situations (*7*, *18*). We shall follow the same procedure in most of our analysis here and adopt the same approach for the particle velocity and dispersivity. Note, however, that in real situations it is essential to verify that contributions from dispersion are indeed small. In all cases studied here, the correction terms in the above equations contribute no more than 10%.

Materials and Methods

Natural Porous Medium. The soil material used was collected from a noncalcareous soil in northern Switzerland

(Riedhof soil, dystric Eutrochrept). The soil material had silt loam texture, contained 6 g/kg total carbon and 10 g/kg dithionite extractable iron, and had a cation exchange capacity of 70 mmol/kg. The mineralogy of the soil was dominated by quartz, vermiculite, illite, and kaolinite, with traces of chlorite and goethite. Additional details on the soil chemical characteristics are given elsewhere (*1*, *19*).

The collected soil material was thoroughly mixed to generate a homogeneous batch, sieved to pass a 2-mm screen, air-dried, and stored at 4 °C. Soil aggregates ranging from 1.0 to 2.0 mm in diameter, separated by dry sieving, were dry packed into chromatographic glass columns (Omnifit, Cambridge, UK). The columns were purged with CO_2 gas and then water-saturated by slowly pumping a 0.5 M $CaCl_2$ solution in the upward direction. Following packing and water saturation, the columns were preconditioned by leaching about 200 pore volumes of 0.5 M $CaCl_2$ solution. For experiments involving particle deposition with NaCl solutions, the columns were further preconditioned with an additional 1000 pore volumes of 0.5 M NaCl solution until the calcium concentration dropped below 10^{-7} M.

Colloidal Particles. The majority of the column transport experiments were carried out with in situ mobilized soil colloidal particles. Mobile particles were obtained by collecting colloidal suspensions during independent release experiments from the same soil material used in the column transport experiments. Columns preconditioned with $CaCl_2$ (see above) were completely sodium saturated by leaching with about 1000 pore volumes of 0.5 M NaCl. Following this step, the ionic strength was reduced by feeding the column with a 0.02 M NaCl solution. This ionic strength reduction initiated the release of colloidal particles, resulting in soil particle concentrations at the column outlet as high as about 100 mg/L. The mobilized colloidal particles suspended in the collected column effluent were subsequently concentrated by flocculation with 0.5 M $CaCl_2$ solution. The flocculated particles were then Na-saturated, subsequently dialyzed extensively against deionized water, and stored in the dark at 4 °C.

In addition to the natural particles, experiments with monodisperse colloidal latex microspheres were also carried out to further explore the particle transport behavior in the packed soil columns. Highly charged, fluorescent polystyrene latex particles with carboxyl functional groups (Interfacial Dynamics Corporation, Portland, OR) were used as a surrogate to natural colloidal particles. The negatively charged carboxyl modified latex particles had a mean diameter of 0.11 μm and a surface charge density of 65.1 $\mu C/cm^2$. In addition, a suspension of positively charged latex particles with amidine functional groups was used to test the deposition rate under favorable chemical conditions. The positively charged particles had a mean diameter of 0.12 μm and a surface charge density of 8.1 $\mu C/cm^2$.

Characterization of Colloids. The size and morphology of the in situ mobilized colloidal particles were studied by transmission electron microscopy (TEM). Particle size was also estimated by dynamic light scattering measurements using an ALV goniometer (ALV/SP-125 S/N 30, ALV, Langen, Germany) equipped with a krypton laser (Innova 300, Coherent) operating at a wavelength of 647 nm. Second cumulant fits of the correlation function were used to estimate the hydrodynamic diameter of the particles as described elsewhere (*20*). The mineralogical composition of the mobile soil colloidal particles was determined by X-ray diffraction analysis (Scintag XRD 2000). Samples were saturated with K^+ or Mg^{2+} and analyzed either untreated, heated to 550 °C, or saturated with ethylene glycol. Electrophoretic mobilities of the particles were determined by microelectrophoresis with a laser Doppler velocimetry apparatus (ZetaSizer 3, Malvern). Triplicate measurements were obtained with an applied electric field of 30 V/cm, 30 s count time, and a modulator frequency of 1 kHz.

Column Setup. The column setup used for the particle transport includes a reservoir containing the background electrolyte solution, a degasser, a high-pressure HPLC pump, a chromatography glass column packed with the soil material, a pulse injection loop at the column inlet, and a flow through detector system. Feed solution was pumped by an HPLC pump through a degasser into the column in a upward flow. Colloidal particles or tracer were injected by an injection loop, and the concentration at the column outlet was monitored on-line using a flow-through detection system as described below. Column dimensions for the various particle transport experiments ranged from 1.0 to 2.5 cm in diameter and 6−46 cm in length. More details on the column setup can be found in Kretzschmar et al. (*7*).

Tracer Experiments. Characteristics of the soil columns, such as pore volume and tracer dispersivity, were determined from pulse experiments using NO_3^- as a conservative tracer. Short pulses of $Ca(NO_3)_2$ solutions were injected with a sample loop (96 μL) into a $CaCl_2$ background column feed solution. Nitrate breakthrough was monitored on-line with an HPLC UV−vis detector (Linear) at a wavelength of 220 nm. The mean travel time of the nonreactive tracer and the dispersion coefficient were obtained either by evaluating the first and second moments of the tracer breakthrough or by fitting the breakthrough data to the advection dispersion equation, as described in the theoretical section. Both methods yielded practically identical results. The effect of fluid flow velocity on the observed dispersivity was investigated by systematically varying the pore water velocity from 1.8×10^{-5} to 5.4×10^{-4} m/s.

Particle Transport Experiments. Particle transport experiments were conducted by injection of 96-μL pulses of sonicated, well dispersed colloidal suspensions at a room temperature of 24° ± 1 C. An HPLC UV−vis detector set to a wavelength of 250 nm was used for transport experiments with the natural soil colloidal particles. The fluorescent carboxyl latex particles were measured by an HPLC fluorescence detector operating at excitation and emission wavelengths of 490 and 515 nm, respectively. The residual (background) colloid concentrations at the column outlet were estimated by elemental analysis of the effluent and for most experimental conditions were below 0.07 mg/L. Total amounts of injected particles n_0 were determined from separate bypass experiments where the column was short-circuited. In all column experiments, the bulk density of the packed soil was 0.92 g/cm^3, and the resulting porosity was 0.61. Several sets of column experiments were carried out as described below.

In the first set of experiments, the general characteristics of the transport behavior of the natural colloidal particles in their parent soil matrix were investigated. Additional experiments were conducted with monodisperse carboxyl latex particles to compare their transport behavior to that of the heterogeneous natural colloidal particles. The columns used for this set of experiments were 46 cm long and had an inner diameter of 1.0 cm. After the standard preconditioning of the packed soil as described earlier, the soil columns were equilibrated with 0.3 mM $CaCl_2$ for several pore volumes. Duplicate column experiments were performed to confirm reproducibility.

To verify the assumption of first-order deposition kinetics in the packed soil columns, a second set of transport experiments was conducted. In this set of experiments, the amount of colloidal particles injected to the column feed solution varied from 32 to 258 μg. The column used for this series of experiments was 2.4 cm in diameter and 45 cm in length. After equilibrating the column with 0.3 mM $CaCl_2$, the flow rate was adjusted to 2.45×10^{-4} m/s. All column

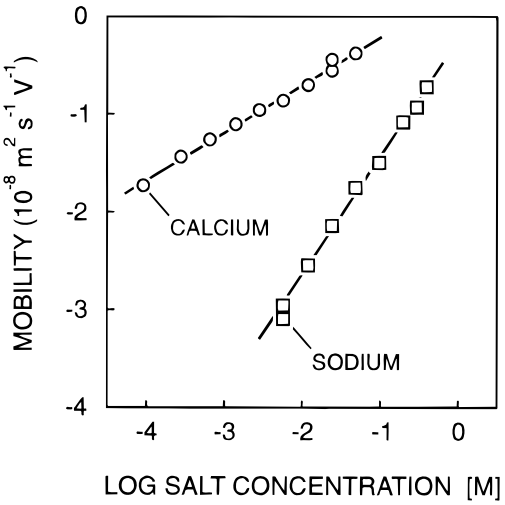

FIGURE 1. Electrophoretic mobility of the in situ mobilized soil particles as a function of Na^+ and Ca^{2+} concentration. Temperature was maintained at 25 °C and solution pH was 5.7 ± 0.1.

runs in this set of experiments were conducted with an electrolyte concentration of 0.3 mM $CaCl_2$.

In the third set of experiments, the effect of fluid flow velocity on the deposition kinetics and dispersivity of the natural and carboxyl latex particles was investigated. In these experiments, the pore water velocity was systematically varied from 1.8×10^{-5} to 5.4×10^{-4} m/s. Columns were 46 cm long and with inner diameters ranging from 1.0 to 2.4 cm in order to extend the accessible range of pore water velocities. These experiments were performed with a background electrolyte concentration of 0.3 mM $CaCl_2$.

The last set of experiments was carried out to study the effect of solution chemistry on the deposition kinetics of the natural and synthetic latex colloidal particles. The effect of electrolyte concentration, counterion valence (Na^+ versus Ca^{2+}), and solution pH were investigated. The electrolyte concentration (NaCl or $CaCl_2$) was varied from 0.1 to 800 mM. Prior to the deposition experiments, columns were presaturated with the corresponding electrolytes. To investigate the effect of solution pH, columns were fed with azide-buffer solutions adjusted to various pH values by HCl. The columns were equilibrated with the buffer solution until the column effluent pH approached the feed solution pH. The inner diameter of the columns in the deposition kinetics experiments was kept constant (1.0 cm), but the column length varied from 6 to 46 cm to allow measurements of a wide range of collision efficiencies (or deposition rate coefficients). All column runs in this set of experiments were conducted at a constant flow rate of 3.6×10^{-4} m/s.

Results and Discussion

Properties of Porous Medium and Colloidal Particles. The dynamic light scattering results and TEM images revealed that the in situ mobilized soil colloidal particles were highly polydisperse and irregular in shape. These measurements showed that the upper limit of the size distribution was about 1 μm. The X-ray diffraction analysis confirmed that the soil particles were also highly heterogeneous in their mineralogical composition, which was similar to that of the total clay fraction.

The electrophoretic mobility of the soil particles as a function of Na^+ and Ca^{2+} concentration is shown in Figure 1. As expected, the electrophoretic mobility of the soil colloidal particles decreases when the salt concentration is increased, and the reduction in the electrophoretic mobility is much more pronounced with the divalent Ca^{2+} counterions than with the monovalent Na^+ counterions. Because the in

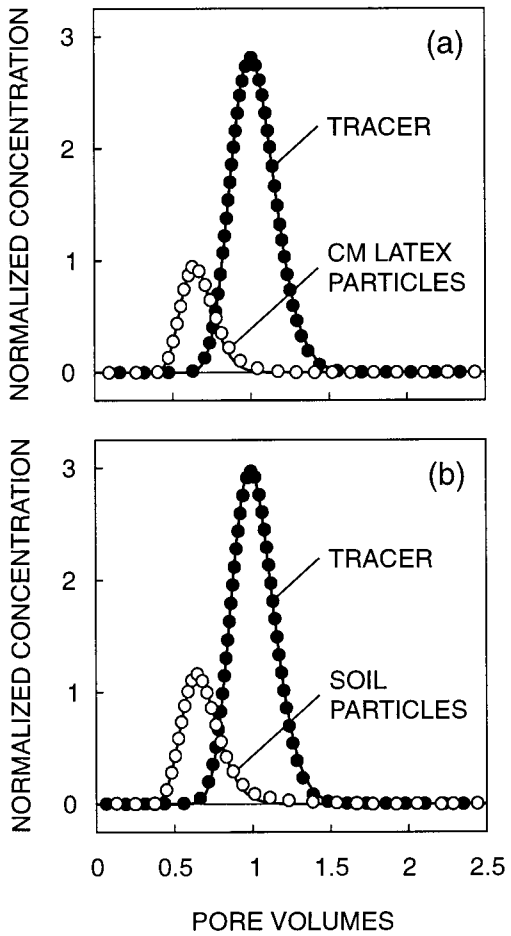

FIGURE 2. General particle transport behavior in the packed soil column resulting from pulse input experiments. (a) Breakthrough curves of the carboxyl modified (CM) latex particles (○) compared to a nonreactive tracer (●). (b) Breakthrough curves of the natural soil colloidal particles (○) compared to a nonreactive tracer (●). Solid lines correspond to the breakthrough curves obtained by fitting eq 2 to the experimental curves. Particle transport experiments were carried out with a background electrolyte concentration of 0.3 mM $CaCl_2$.

situ mobilized soil colloidal particles have similar chemical properties as the soil parent aggregates, the measured electrophoretic mobility of the soil particles is indicative of the electrostatic double layer interaction that would develop between the colloidal particles and the soil aggregates during the particle transport experiments. The electrophoretic mobility data of Figure 1 will be used later to explain the particle deposition kinetics behavior with of Na^+ and Ca^{2+}.

General Particle Transport Behavior. Particle and tracer breakthrough curves for the soil and carboxyl latex particles are depicted in Figure 2. Best fits obtained from the advection-dispersion equation (eq 2), with optimized values of v, D, and k, are also shown (solid lines). Inspection of the breakthrough curves in Figure 2 immediately reveals two distinct features. First, particle breakthrough occurs much earlier than the solute tracer; that is, colloidal particles in the soil column travel considerably faster than a nonreactive tracer. Second, only a fraction of the injected particles is recovered at the column effluent, as indicated by the reduced peak and area of the normalized particle breakthrough compared to that of a tracer.

The faster transport of colloidal particles compared to that of a conservative tracer is attributed to the phenomenon of size exclusion (*7*). Contrary to the nonreactive solute, a portion of the pore space of the soil matrix is not accessible

TABLE 1. Particle Transport Parameters Determined from Curve Fitting and Moment Analysis of the Particle and Tracer Breakthrough Curves Shown in Figure 2[a]

	curve fitting			moment analysis		
	velocity[b] (m/s)	dispersion[c] (m^2/s)	deposition rate coeff[d] (h^{-1})	velocity[b] (m/s)	dispersion[c] (m^2/s)	deposition rate coeff[d] (h^{-1})
CM latex particles	1.0×10^{-4}	5.1×10^{-7}	1.44	1.1×10^{-4}	6.2×10^{-7}	1.37
tracer	7.0×10^{-5}	2.4×10^{-7}		6.9×10^{-5}	2.4×10^{-7}	
soil particles	1.0×10^{-4}	7.7×10^{-7}	0.76	1.1×10^{-4}	1.2×10^{-6}	0.72
tracer	7.1×10^{-5}	2.9×10^{-7}		7.1×10^{-5}	3.0×10^{-7}	

[a] Estimates of the average relative error based on independent replicates are given as footnotes. [b] Average relative error <10%. [c] Average relative error <20%. [d] Average relative error <30%.

to the mobile colloidal particles. In this physical mechanism of size exclusion, the pores through which particles cannot travel are basically those which are smaller than the colloidal particles. Other physicochemical processes related to particle interaction with soil grain surfaces may also cause an apparent size exclusion. Because particle-grain collision frequency increases as pores become narrower, the major fraction of colloidal particles detected at the column outlet originates from colloidal particles which traveled through large pores. In addition, as can be inferred from the moment analysis presented in the theoretical section, the occurrence of particle deposition in combination with hydrodynamic dispersion results in a shift of the center of mass of the particle breakthrough curves toward smaller times.

The second distinct feature of the particle breakthrough curves in Figure 2—the reduced peak height and area of the normalized particle breakthrough compared to that of a solute tracer—is attributed to immobilization of colloidal particles on the surfaces of soil grains due to particle deposition. Barring changes in solution chemistry and fluid flow rate, particle deposition results in irreversible attachment of colloidal particles. The rather good fits of the experimental data to the advection-dispersion equation with a first-order irreversible particle deposition term supports this assertion of irreversible particle deposition. It must be emphasized that irreversibility of particle deposition does not merely imply an absolute immobilization of colloidal particles, but rather it means that particle deposition rate is much larger than particle release. In this context, it is worth noting the very small tailing observed in the particle breakthrough curves when compared with the fits to the advection dispersion equation. This behavior may be attributable to deposition and subsequent release of colloidal particles.

It is striking that the general transport behavior of the natural and carboxyl latex particles shown in Figure 2 appears similar, despite the large variability in physical and chemical properties of the natural colloidal particles. However, close inspection of the estimated particle transport parameters *v*, *D*, and *k* (Table 1) indeed shows that the different physical and chemical properties of the natural colloidal particles compared to those of the carboxyl modified latex particles result in differences between the transport parameters, particularly in the values of the particle deposition rate coefficient *k*.

A key assumption in modeling particle transport in porous media is that particle deposition follows first-order kinetics. This assumption pertains to the initial stages of deposition, before blocking or ripening effects become important (*10*), which is the case in our experiments where very small amounts of particles are introduced to the column. Figure 3 presents particle breakthrough curves of experiments with various input masses of colloidal particles, ranging from 32 to 258 μg. As shown, the different breakthrough curves are identical, thus providing an unequivocal proof that the deposition of the heterogeneous natural colloidal particles is a linear process which follows first-order kinetics.

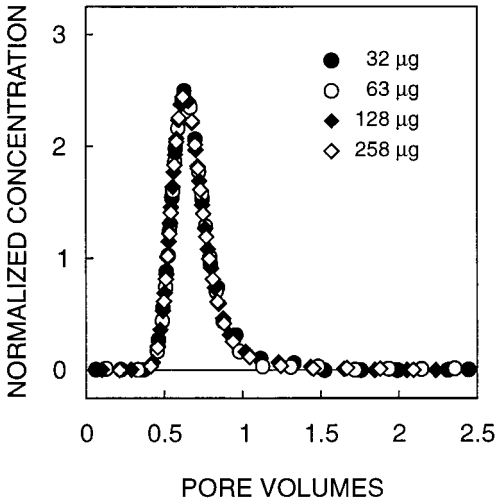

FIGURE 3. Normalized breakthrough curves of the natural colloidal particles (with 0.3 mM $CaCl_2$) for different initial amounts of colloidal particles (μg) introduced to the column inlet (pulse input). Pore water velocity during the experiments was maintained at 2.45 $\times$ 10^{-4} m/s.

Although not directly evident from Figure 2, it is worthwhile to note that the hydrodynamic dispersion of colloidal particles is greater than that of the nitrate tracer. This can be seen by comparing the values of *D* (Table 1) obtained from fitting the advection-dispersion equation to the experimental data. This finding, along with the other two major features of size exclusion and reduced amount of particles at the effluent due to particle deposition, is subject of a more thorough analysis in the following subsections.

Physical Aspects of Particle Transport. The dependence of the relative particle velocity (i.e., the ratio of particle to tracer velocities) on pore water velocity for the soil and carboxyl modified latex particles is presented in Figure 4a. As discussed earlier, colloidal particles in the packed soil column travel faster than a conservative tracer due to size exclusion effects. The data in Figure 4a demonstrates that, for the given soil, colloidal particles travel about 1.45 times faster than a conservative tracer, regardless of changes in pore water velocity over nearly 2 orders of magnitude. This behavior points out that the inaccessibility of small pores in the soil aggregates to colloidal particles does not change with variations in pore water velocity and that size (volume) exclusion is the main cause of the particle velocity enhancement. Under the chemical and physical conditions investigated, other factors which depend on pore water velocity (e.g., particle deposition) and that may result in apparent size exclusion play a negligible role.

Figure 4b describes the variation of the particle and tracer dispersivities as a function of pore water velocity. The slope of the dispersivity versus pore water velocity curves (on a log—log scale) for the colloidal particles (both natural and

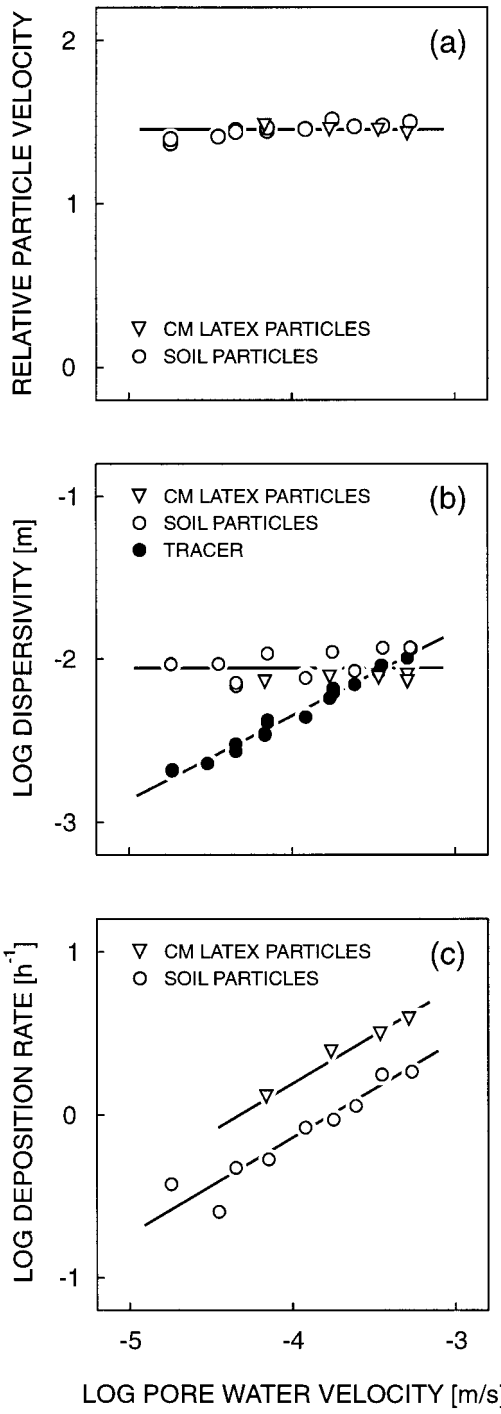

FIGURE 4. Influence of flow velocity on the transport characteristics of colloidal particles in the packed soil column. (a) Change of the relative particle velocity (i.e., ratio of particle to tracer velocity) as a function of pore water velocity for the soil and the carboxyl modified (CM) latex particles. (b) Influence of flow velocity on the dispersivities of the soil and CM latex particles compared to the tracer dispersivity. (c) Influence of flow velocity on the deposition rate of the soil and CM latex particles. Particle transport experiments were carried out with a background electrolyte concentration of 0.3 mM $CaCl_2$.

carboxyl modified latex particles) is zero, while that for the tracer is 0.6. These values correspond to slopes of dispersion coefficient versus pore water velocity (log−log scale) of 1.0 and 1.6 for the particles and tracer, respectively. The results further demonstrate that the tracer dispersivity is smaller than that of the colloidal particles over nearly the entire range of pore water velocities investigated. It should be emphasized that the obtained dispersion coefficients are valid for the column scale. Scale dependence of dispersivity, though beyond the scope of this paper, should be considered when analyzing solute or particle dispersivities at the field scale.

When analyzing the dependence of the dispersion coefficient on pore water velocity it is customary to present the data as D/D_0 versus the Peclet number Pe. In this analysis D is the longitudinal dispersion coefficient, and D_0 is the molecular diffusion of the solute tracer or the Brownian diffusion coefficient based on Stokes−Einstein relation for the colloidal particles. The Peclet number Pe is defined as $v_0 d_g/D_0$, with d_g being the grain diameter and v_0 the pore water velocity. Experimental data for laminar flow usually display four dispersion regimes as described below (*21*, *22*).

The first is the diffusion regime (for Pe < 0.3) where advection is negligible and diffusion is the sole contribution to dispersion. The second regime, for 0.3 < Pe < 5, is a transition regime where advection starts to contribute to dispersion and D/D_0 appears to increase with Pe. These two dispersion regimes, however, are for Peclet numbers much smaller than those relevant to our experiments in Figure 4b. In the third regime (5 < Pe < 300), the so-called power-law regime, advection dominates dispersion, and D/D_0 is proportional to Pe^m, with $m \approx 1.2$ based on available experimental data. Koch and Brady (*21*) denoted this regime as the boundary-layer dispersion, since it is suggested that in this regime diffusion transfers materials from very slow regions near the grain surfaces to faster streamlines. The fourth regime (300 < Pe < 10^5) is the regime of mechanical dispersion. In this case, dispersion is caused by the stochastic velocity field induced by the randomly distributed pore boundaries. Dimensional analysis for this regime of mechanical dispersion indicates that $D/D_0 \sim$ Pe. Another dispersion regime, usually denoted as holdup dispersion, is found when solutes are trapped in dead-end regions or within pores in the solid grains, from which they can escape only by molecular diffusion (*21*−*23*). In this region $D/D_0 \sim Pe^2$, which indicates a stronger dependence of dispersion on the Peclet number.

The Peclet numbers of our experimental data in Figure 4b fall in the fourth regime (300 < Pe < 10^5) for the colloidal particles and in the third (5 < Pe < 300) and fourth (300 < Pe < 10^5) regimes for the tracer dispersion. Hence, the dependence of the dispersivity of the colloidal particles on the pore water velocity is as expected for the region of pure mechanical dispersion (i.e., $D/D_0 \sim$ Pe or slope zero for the curve of log dispersivity versus log pore water velocity). As for the tracer solute, the experimental data display $D/D_0 \sim Pe^{1.6}$. At the lower pore velocities used in Figure 4b, Pe is in the power-law regime, while for the higher pore velocity data Pe is in the mechanical dispersion regime. Thus, the experimental observation of $D/D_0 \sim Pe^{1.6}$ cannot be explained by simple mechanical or advection dominated dispersion. It is most likely that holdup dispersion where theoretical analyses show $D/D_0 \sim Pe^2$ also takes place. This is in particular relevant for the soil aggregates since our earlier data point out the existence of an excluded pore volume which is contributed by small pores within the soil aggregates. Because tailing in the tracer breakthrough data was not prominent, we conclude that mechanical dispersion as well as hold up dispersion take place within the soil aggregates, which results in a power-law dependence that is between 1 and 2.

The effect of pore water velocity on the deposition rate coefficient of the soil and carboxyl modified latex particles is presented in Figure 4c. As shown, particle deposition rate coefficients increase with increasing pore water velocity. The slope of the log k versus log v_0 curves for both the soil and latex particles is 0.6. This slope is somewhat higher than

what predicted by fundamental theories of particle deposition onto impermeable solid surfaces, such as spherical collector grains. For particles smaller than about 1 μm, where particle deposition is controlled by convective diffusion, the deposition rate coefficient is dependent on the pore water velocity to the power of one-third, i.e., $k \propto v_0^{1/3}$ (*8*, *10*). Song and Elimelech (*24*) extended this analysis to particle deposition onto permeable surfaces. For permeable (porous) surfaces which allow the passage of fluid molecules through the pores but block the transport of colloidal particles, the deposition rate coefficient is controlled by the convective particle transport, that is $k \propto v_0$. The breakthrough curves of the tracer and colloidal particles shown earlier in Figure 2 indicate that the soil aggregates are porous and that, in contrast to the tracer molecules, colloidal particles cannot travel through the pores. Hence, for the data shown in Figure 4c, the dependence of the measured deposition rate coefficient on pore water velocity ($v_0^{0.6}$) is between what is expected for deposition onto impermeable surfaces ($v_0^{1/3}$) and permeable, porous surfaces ($v_0^{1.0}$).

Effect of Solution Chemistry on Particle Deposition Kinetics. Particle deposition kinetics in natural and engineered systems are markedly influenced by the solution chemistry. Divalent cations, such as Ca^{2+} and Mg^{2+}, are important constituents of soils and natural waters. These ions play a significant role in controlling the stability, reactivity, and fate of colloidal particles in aquatic environments.

The deposition kinetics of the soil and synthetic latex particles as a function of Na^+ and Ca^{2+} concentrations are depicted in Figure 5. Results are presented as stability curves: that is, the logarithm of the deposition rate coefficient k, or the collision efficiency α, as a function of the logarithm of counterion concentration. The collision efficiency is defined as k/k_{fast}, where k_{fast} is the value of k for favorable deposition (i.e., for counterion concentration at or above the critical deposition concentration). The results demonstrate that calcium ions have a much more pronounced effect on the kinetics of particle deposition than sodium ions. Substantial particle deposition occurs at a much lower concentration of Ca^{2+} than Na^+. The critical deposition concentrations for Ca^{2+} (ca. 5 and 2 mM for the natural and latex particles, respectively) are much lower than those with Na^+ (ca. 200 mM for both the soil and latex particles). From the experiments with the azide buffer it is seen that pH has no measureable effect on the deposition rate in the pH range 4.0−5.5. It is also rather remarkable that the colloid stability curves of the soil colloidal particles (Figure 5a) are quite alike those of the synthetic latex particles (Figure 5b), and other stability curves displayed in previously published studies with model particles and collectors (*10*, and references therein), despite the marked heterogeneity of the soil colloidal particles in terms of chemical composition, particle size, and morphology.

The deposition behavior with Na^+ and Ca^{2+} shown above is generally in qualitative agreement with the classical Derjaguin, Landau, Verwey, and Overbeek (DLVO) theory of colloidal stability and the well-known Schulze−Hardy rule (*25*), whereby divalent counterions reduce colloidal stability much more effectively than monovalent counterions. The dependence of the particle deposition kinetics on Na^+ and Ca^{2+} concentrations is also in qualitative agreement with the effect of these counterions on the electrophoretic mobility of the particles, as was shown earlier in Figure 1. It is clear from the results in Figure 1 that the divalent counterions are much more effective in lowering the particle electrokinetic charge and, hence, in reducing colloidal stability than the monovalent counterions.

An important feature of colloid stability curves, in addition to the critical deposition concentration, is the slope

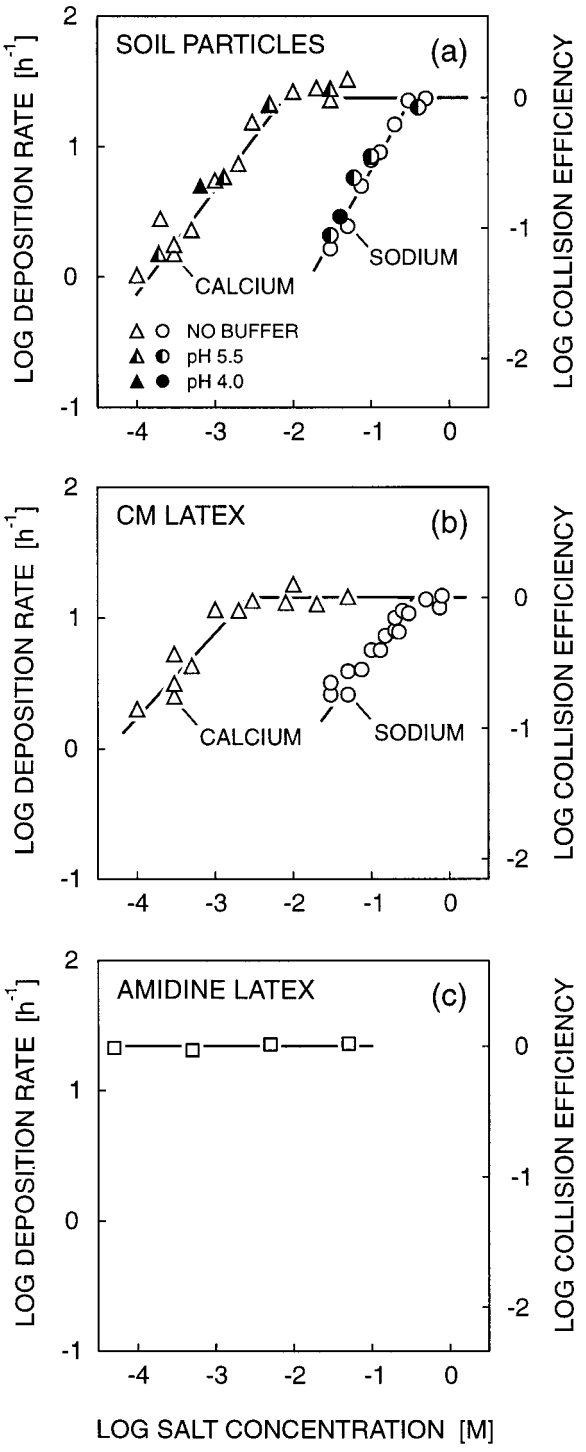

FIGURE 5. Influence of solution chemistry on particle deposition kinetics in the packed soil columns. (a) Effect of electrolyte (NaCl or $CaCl_2$) concentration, counterion valence (Na^+ and Ca^{2+}), and solution pH (pH 4.0 or 5.5, controlled by azide buffer) on deposition rate coefficients and experimental collision efficiencies for the soil particles. (b) Influence of electrolyte concentration and counterion valence on deposition kinetics for the carboxyl modified (CM) latex particles. (c) Influence of electrolyte ($CaCl_2$) concentration on deposition kinetics for the positively charged amidine latex particles. All experiments were conducted at a pore water velocity of 3.6 $\times$ 10^{-4} m/s.

$d \log \alpha / d \log C_s$, where C_s is the molar salt concentration. Theoretical analyses based on DLVO theory for deposition of homogeneous, monodisperse colloidal particles onto homogeneous solid surfaces reveal that the slope of the

stability curves decreases with an increase in the valence of the counterions. Another common observation in particle deposition kinetics studies is the much greater slope of predicted stability curves compared with experimentally determined curves (*10*, *13*). The experimental results show that the slopes of the stability curves for Na^+ (1.1 and 0.8 for natural and latex colloids, respectively) are higher than the corresponding slopes with Ca^{2+} (0.8 and 0.6 for the natural and latex particles, respectively). It must be emphasized that our discussion here is rather qualitative, since a quantitative analysis based on DLVO theory is not meaningful for the highly heterogeneous natural porous media and natural soil colloidal particles used.

At electrolyte levels above the critical deposition concentration, the particle deposition rate coefficient attains its maximum value (k_{fast}), and further increases in electrolyte concentration do not affect the deposition rate. Under these conditions, electrostatic double layer repulsion is eliminated, and particle deposition rate is transport limited. Based on the data in Figure 5a,b, the measured k_{fast} values for the carboxyl latex particles and soil colloidal particles are 15 and 22 h^{-1}, respectively. The value of k_{fast} for the 0.11 μm carboxyl modified latex particles is comparable to that obtained with 0.12 μm positively charged amidine latex particles as shown in Figure 5c (average of the four data points is 15 h^{-1}). For deposition with the positively charged latex particles, double layer interactions are attractive, and particle deposition rate is transport limited.

Use of Filtration Theory for Predicting Particle Deposition Kinetics. Filtration theory has been quite successful in predicting favorable particle deposition rates in model porous media, such as glass beads and well sorted sand grains (*10*). At this writing, it is yet to be shown that filtration theory is applicable to heterogeneous and complex natural porous media, such as the soil matrix used in this study. Here we will compare predictions based on filtration theory with the favorable deposition rate coefficients obtained with the 0.12 μm positively charged amidine latex particles (Figure 5c). Using a pore water velocity of 3.6×10^{-4} m/s for the relevant column experiments, a particle velocity (v) of 1.45 times the pore water velocity (Figure 4a), and the other relevant experimental conditions, the particle deposition rate coefficient (k) for a given effective grain diameter (d_g) of the soil matrix can be calculated from (*7*, *10*)

$$k = \lambda v \tag{7}$$

$$\lambda = \frac{3}{2}\frac{1-f}{d_g}\eta \tag{8}$$

Here, f is the effective porosity of the granular porous medium, λ is the filter coefficient, and η is the single collector efficiency. Our calculations show that the favorable particle deposition rate coefficient is 11 h^{-1} for an effective grain size of 1 mm (lower size range of the soil matrix) and 6 h^{-1} for an effective grain size of 2 mm (upper size range). Considering the profound physical heterogeneity of the soil matrix, these values compare rather well with the average experimental value of 15 h^{-1} obtained in Figure 5c and to the k_{fast} values of 15−22 h^{-1} obtained in Figure 5a,b for the soil and CM latex particles. One should note, however, that these calculations pertain to the favorable particle deposition regime. No theoretical methods are available to predict the deposition rate coefficients under the more relevant unfavorable chemical conditions. In the latter case, one has to rely on experimental determination of the deposition rate coefficients as outlined earlier in this paper.

Acknowledgments

The work described in this paper was conducted at the Swiss Federal Institute of Technology (ETH). The hospitality and support of ETH during the sabbatical of one of the authors (M.E.) at the Institute of Terrestrial Ecology is greatly appreciated.

Literature Cited

(1) Grolimund, D.; Borkovec, M.; Barmettler, K.; Sticher, H. *Environ. Sci. Technol.* **1996**, *30*, 3118−3123.
(2) McCarthy, J. F.; Zachara, J. M. *Environ. Sci. Technol.* **1989**, *23*, 496−502.
(3) Ryan, J. N.; Elimelech, M. *Colloids Surf. A* **1996**, *107*, 1−56.
(4) McCarthy, J. F.; Degueldre, C. In *Environmental Particles*; van Leeuwen, H. P., Buffle, J., Eds.; Lewis Publisher: Chelsea, MI, 1993; pp 247−315.
(5) Jenny, H.; Smith, G. D. *Soil Sci.* **1935**, *39*, 377−389.
(6) Khilar, K. C.; Fogler, H. S. *J. Colloid Interface Sci.* **1984**, *101*, 214−224.
(7) Kretzschmar, R.; Barmettler, K.; Grolimund, D.; Yan, Y.; Borkovec, M.; Sticher, H. *Water Resour. Res.* **1997**, *33*, 1129−1137.
(8) Song, L.; Elimelech, M. *J. Chem. Soc., Faraday Trans.* **1993**, *89*, 3443−3452.
(9) de Marsily, C. *Quantitative Hydrology*; Academic Press: San Diego, CA, 1986.
(10) Elimelech, M.; Gregory, J.; Jia, X.; Williams, R. A. *Particle Deposition and Aggregation. Measurement, Modelling, and Simulation*; Butterworth-Heinemann: 1995.
(11) Litton, G. M.; Olson, T. M. *Colloids Surf. A* **1994**, *87*, 39−48.
(12) Kallay, N.; Nelligan, J. D.; Matijevic, E. *J. Chem. Soc., Faraday Trans. 1* **1983**, *79*, 65−74.
(13) Elimelech, M.; O'Melia, C. R. *Environ. Sci. Technol.* **1990**, *24*, 1528−1536.
(14) Vinten, A. J. A.; Nye, P. H. *J. Soil Sci.* **1985**, *36*, 531−541.
(15) Kretzschmar, R.; Robarge, W. P.; Amoozegar, A. *Environ. Sci. Technol.* **1994**, *28*, 1907−1915.
(16) Jury, W. A.; Roth K. *Transfer Functions and Solute Movement Through Soils: Theory and Applications*; Birkhauser Verlag: Basel, Switzerland, 1990.
(17) Villermaux, J. In *Percolation Processes: Theory and Applications*; Rodrigues, A. E., Tondeur, D., Eds.; Sijthoff & Noordhoff: Alphen aan den Rijn, The Netherlands, 1981; pp 83−140.
(18) Harmand, B.; Rodier, E.; Sardin, M.; Dodds, J. *Colloids Surf. A* **1996**, *107*, 233−244.
(19) Grolimund, D. Ph.D. Dissertation, Swiss Federal Institute of Technology: Zurich, Switzerland, 1997.
(20) Wu, Q.; Borkovec, M.; Sticher, H. *Soil Sci. Soc. Am. J.* **1993**, *57*, 883−890.
(21) Koch, D. L.; Brady, J. *J. Fluid Mech.* **1985**, *154*, 399−427.
(22) Sahimi, M. *Flow and Transport in Porous Media and Fractured Rocks*; VCH: Weinheim, 1995.
(23) Carberry; Bretton, R. H. *AIChE J.* **1958**, *4*, 367−375.
(24) Song, L.; Elimelech, M. *J. Colloid Interface Sci.* **1995**, *173*, 165−180.
(25) Verwey, E. J. W.; Overbeek, J. Th. G. *Theory of Stability of Lyophobic Colloids*; Elsevier: Amsterdam, 1948.

Received for review April 9, 1998. Revised manuscript received August 24, 1998. Accepted August 27, 1998.

ES980356Z